Study On Grinding Force of High Volume Fraction SiCp/Al2024 Composites

Guangyan GUO（✉ 1282794392@qq.com）

Liaoning Institute of Technology: Liaoning University of Technology

Qi Gao

Liaoning Institute of Technology: Liaoning University of Technology

Quanzhao Wang

Liaoning Institute of Technology: Liaoning University of Technology

Shichao Pan

Liaoning Institute of Technology: Liaoning University of Technology

Study on grinding force of high volume fraction SiCp/Al2024 composites

Guangyan Guo[1]. Qi Gao[1]. Quanzhao Wang[2]. and Shichao Pan[1]

Abstract:

In view of the difficult machining characteristics of high volume fraction SiCp/Al composites, this paper researches the grinding force variation of grinding SiCp/Al composites with grinding rod. A diamond grinding rod with a diameter of 3mm is used to grind the SiCp/Al2024 composite with 60% volume fraction by the method of end face grinding. By measuring the tangential grinding forces and normal grinding forces after grinding, the theoretical model of unit grinding force is deduced. According to the experimental parameters of spindle speed, feed rate and grinding depth, this paper derives the theoretical model of grinding force based on SiCp/Al2024 composites. And it clarifies the influence mechanism of grinding depth and feed rate on grinding force and explores the variation of grinding parameters on grinding force under dry grinding condition. Then the variation rule of grinding component force ratio is obtaines. The related research and theoretical model have theoretical guiding significance for exploring the grinding properties of hard-to-machine materials.

Key words: SiCp/Al composites. Theoretical model. Grinding force. Grinding parameters. Grinding component force ratio

APPEENDIX I

Notation

v_s　　spindle speed

v_w　　feed rate

a_p　　grinding depth

F_t　　tangential grinding forces

F_n　　normal grinding forces

F_p　　unit grinding force

F　　grinding force

C_f　　grinding component force ratio

1. Introduce

With the advent of precision machining technology, grinding technology has become the main processing method of particle reinforced matrix composites. Among composites, SiCp/Al composites have the advantages of high strength, high hardness and so on. Therefore, they have been used in precision optical instruments, advanced weapons and aerospace fields [1-4]. In contemporary academia, many scholars have studied the properties of SiCp/Al composites by using grinding technology [5].

Grinding force is one of the main factors affecting the grinding process, which has been widely studied and researched by scholars. Zhou et al. [6] processed SiCp/Al composites by using ultrasonic vibration-assisted grinding method, and proposed a mechanical model to predict the ultrasonic vibration-assisted grinding force of SiCp/Al composites. The coefficients in the grinding force model were obtained by orthogonal experiment. Sakthi Suba Rajas et al. [7] introduced the application of grey relation analysis (GRA) to optimize the surface grinding

#Qi Gao
qqonline@163.com

1. School of Mechanical Engineering and Automation, Liaoning University of　Technology, Jinzhou, 121001,China.

2. Institute of Metal Research, Chinese Academy of Science, 110016

characteristics of SiCp/Al composites, and designed experiments by Taguchi's L9 orthogonal array to observe the surface roughness and tangential forces. Yin et al. [8] proposed an analytical wear force model for SiCp/Al composites. In order to verify this model, a series of experiments on SiCp/Al composites were carried out. At the same time, the paper revealed the relationship between grinding force and machining parameters. And the change rules of grinding force was obtained with grinding depth and feed rate. Yu et al. [9] experimentally studied the ELID grinding characteristics of SiCp/Al composites by using the surface grinding process. The main conclusions were as follows: with the increasing of grinding depth and feed rate of the table, the normal and tangential grinding forces were increasing significantly. Huang et al. [10] carried out grinding experiments on SiCp/Al composites under four grinding conditions, and studied the effects of grinding depth and feed rate on grinding force and grinding component force ratio. Zhao et al. [11] established a grinding simulation model of SiCp/Al composites by carrying out plane grinding experiments with high volume fraction, and studied the influence of feed rate and grinding depth on grinding force.

In addition, Duan et al. [12] conducted cutting experiments on 50% SiCp/Al composites in order to explore the cutting force characteristics of SiC particles reinforced aluminum matrix composites with high volume fraction, analyzed the influence of cutting parameters on the size and fluctuation of cutting force, and studied the relationship between chip formation and cutting force. Pramanik et al. [13] proposed a mechanical model to predict the cutting force of SiCp/Al composites, and explained that the causes of force generation mainly include three aspects: chip formation force, plough-cutting force, and particle fracture force. The chip forming force is obtained by Merchant, and the chip forming force caused by matrix plowing deformation and particle fracture is calculated by the slip line plastic field theory and Griffith fracture theory respectively. Bian et al.

[14] adopted the orthogonal experimental design method and used PCD tools to carry out high-speed cutting experiments on SiCp/Al2009 composites with different volume fraction ratios. Based on the measurement of cutting force and chip thickness, the prediction models of shear Angle, shear stress and friction Angle were established, and the prediction model of cutting force was established based on the basic theoretical formulas of metal cutting. Through cutting experiments of SiCp/Al2024 composites, Han et al. [15] explained the influence of cutting force of cutting material, cutting dosage, content and particle size of SiC on the reinforcing matrix, founded that the phenomenon that the cutting depth component and feed component are greater than the main cutting force will appear by cutting with K type cemented carbide tools when the volume fraction of the enhancement basis is above 18%. In order to accurately predict the cutting force of SiCp/Al composites, Liu et al. [16] proposed a novel cutting force prediction model. In this model, according to the cutting characteristics, SiCp/Al composites with volume fraction of 40% were used for cutting experiments. The results showed that the cutting force model can accurately predict the cutting force under certain cutting parameters.

It can be seen from the above literatures that most scholars adopted the method of macroscopic grinding of low volume fraction SiCp/Al composites to study the influence of its grinding force on the surface of the grinding materials, and established a simulation model to verify the importance of the experimental results. However, most scholars lack of in-depth derivation of grinding force model in mesoscopic grinding process. In this experiment, SiCp/Al2024 composites with reinforced base particles of 60% are used for end grinding. Through 29 groups of single factor experiments, the grinding forces generates in the grinding process are deeply analyzed. And the influence of grinding depth and feed rate on grinding force is summarized. In addition, this paper describes the change of

grinding force under dry grinding condition, and summarizes the change rule of grinding force component force ratio.

2. Experiment design

2.1 Experiment condition

The workpiece material is SiCp/Al2024 composite material, and the volume ratio of SiC particles is 60%. The hardness is high and the processing is difficult. The material characteristics of the workpiece are shown in Table 1.

Table 1 Workpiece material characteristics.

Name	Value
Density ρ (kg/m^3)	2970
Thermal diffusivity (m^2/s)	9.93×10^{-5}
Specific heat (J·kg^{-1}·K^{-1})	689
Thermal conductivity (W·m^{-1}·K^{-1})	203
Young´s modulus (GPa)	206
Poisson´s ratio	0.24
Thermal expansion coefficient (℃$^{-1}$)	7.98×10^{-6}

The processing equipment is Beijing Fine Carver400GA CNC machine tool. The size of the worktable is 490 mm× 430 mm. The maximum rotational speed of the spindle can reach 30000 rpm, the positioning accuracy of x/y/z axis is 0.008/0.008/0.006 mm, the re-positioning accuracy of x/y/z axis is 0.005/0.005/0.005 μm, and the maximum feeding rate of grinding rod is 6 m/min. The micro-grinding experimental platform is shown in Figure 1. The micro-grinding system consists of a carving machine, a grinding rod, a workpiece table and a tool setting instrument. The grinding force collection equipment is high-precision dynamometer and DJ-CL-2 high-precision linear amplifier for three-direction force, as shown in Fig. 2.

Fig. 1 Schematic diagram of grinding experiment system

Fig. 2 Schematic diagram of force measuring system

The specimen is a rectangular block shape of 50 mm × 20 mm × 15 mm. The machinated surface and microstructure of the material are shown in Figure 3.
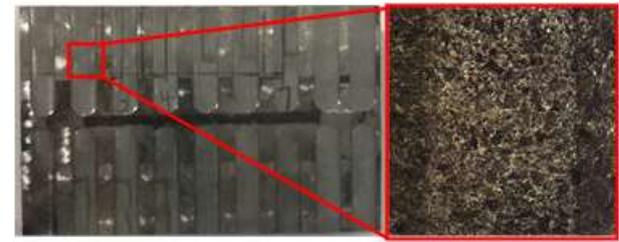

Fig. 3 Machined surface and microstructure

2.2 Experimental procedure

In the experiment, electroplated diamond grinding rod is used to carry out groove grinding experiment on SiCp/Al composites. The diameter of grinding head is 3 mm, the mesh number of grinding rod was #200, and the average grinding particle strength is 150 μm. The grinding process parameters are shown in Table 2.

Table 2 Grinding process parameters

Conditions	Dosage
Grinding rod type	Plated diamond grinding rod #200
Grinding type	Face grinding
Spindle speed v_s/(m/min)	30、35
Feed rate v_w /(m/min)	0.003、0.004、0.005、0.006、0.007
Grinding depth a_p/(mm)	0.01、0.015、0.02、0.025、0.03
Grinding process conditions	Drying grinding

The 29 groups of end face grinding experiments are carried out on the Carver400 high-precision engraving machine. The tangential cutting force (F_t), axial grinding force (F_a) and radial grinding force (F_n) are collected and integrated by the three-direction cutting force experiment system. The specific experiment parameters are shown in Table 3. The grinding process conditions are dry grinding [17-20]. The range of three grinding parameters is that spindle speed (v_s) is 30 or 35 m/min, grinding depth (a_p) is 0.01 mm ~ 0.03 mm, and feed rate (v_w) is 0.003 ~ 0.006 m/min.

Table 3 Parameters of grinding experiment

| Number	v_s /(m/min)	v_w / (m/min)	a_p/ mm
1	30	0.003	0.01
2	30	0.003	0.015
3	30	0.003	0.02
4	30	0.003	0.025
5	30	0.003	0.03
6	30	0.004	0.01
7	30	0.004	0.015
8	30	0.004	0.02
9	30	0.004	0.025
10	30	0.004	0.03
11	30	0.005	0.01
12	30	0.005	0.015
13	30	0.005	0.02
14	30	0.005	0.025
15	30	0.005	0.03
16	30	0.006	0.01
17	30	0.006	0.015
18	30	0.006	0.02
19	30	0.006	0.025
20	30	0.006	0.03
21	30	0.007	0.01
22	30	0.007	0.015
23	30	0.007	0.02
24	30	0.007	0.025
25	30	0.007	0.03
26	35	0.004	0.015
27	35	0.006	0.025
28	35	0.004	0.01
29	35	0.003	0.02

3. Modeling of grinding force

3.1 Mathematical model of unit grinding force

When the abrasive particles begin to contact the workpiece, they will be subjected to the workpiece resistance.Fig. 4 (a) shows the force of the abrasive particles when they are cut into the workpiece surface at the grinding depth. Without considering the friction effect, the cutting force (dF_x) acts vertically on the abrasive cone, and its distribution range is shown in Fig. 4 (b). It can be seen from Fig. 4 (a) that the force is decomposed into normal thrust (dF_{nx}) and lateral thrust (dF_{tx}). The thrust on both sides cancel each other out, while the normal thrust is superimposed to increase the normal force on the whole abrasive grain significantly. Therefore, no matter in which cutting state, the normal force on the abrasive grain is greater than the tangential grinding force.
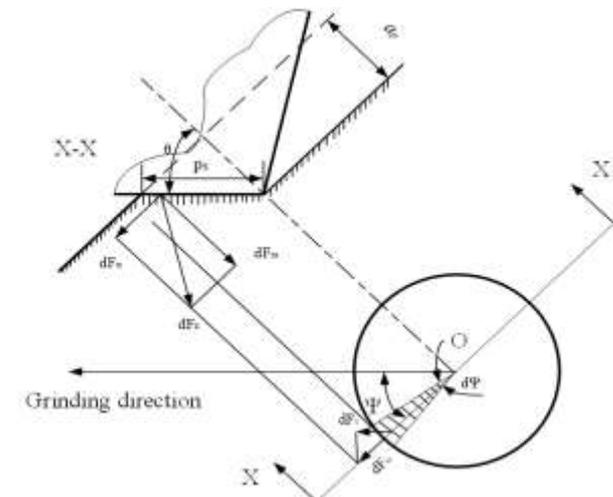
(a)
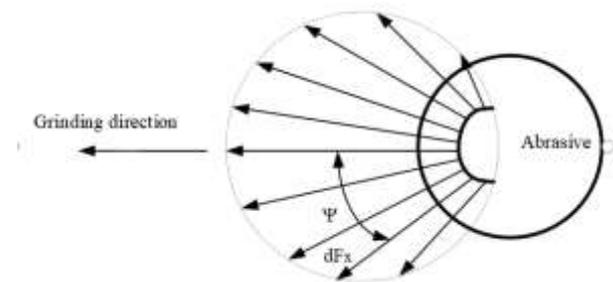
(b)

Fig. 4 Forces on abrasive particles

According to Fig. 4, the cutting force acting on abrasive particles in the X-X cross section can be expressed as:

$$dF_x = F_p dA \cos\theta \cos\psi \qquad (1)$$

Where, F_p is unit grinding force, dA is contact area of grinding rod (the unit is mm^2), θ is half top cone Angle of abrasive grain, Ψ is the included angle between the cutting force direction and the X direction.

The distribution of dF_x is shown in the range of the dotted line in Fig. 4 (b). In the figure, the abrasive particle is a cone with a certain cone Angle, the center line points to the radius of the grinding rod, and the length of the cone bus is ρ. Then the contact area is expressed as:

$$dA = \frac{1}{2}\rho^2 \sin\theta d\Psi \qquad (2)$$

By substituting Equation (2) into Equation (1), the cutting force on the abrasive particles can be expressed as:

$$dF_x = \frac{1}{2}\rho^2 F_p \sin\theta \cos\theta \cos\Psi d\Psi \qquad (3)$$

According to Fig. 4 (a), the following formula can be obtained.

$$\begin{cases} dF_t = dF_x \cos\theta \\ dF_n = dF_x \sin\theta \end{cases} \qquad (4)$$

By substituting the formula (3) into the formula (4), the formula (5) is obtained as follows.

$$\begin{cases} dF_t = \frac{1}{2}\rho^2 F_p \sin\theta \cos^2\theta \cos\Psi d\Psi \\ \\ dF_n = \frac{1}{2}\rho^2 F_p \sin^2\theta \cos\theta \cos\Psi d\Psi \end{cases} \qquad (5)$$

Therefore, the grinding forces acting on the abrasive particles are shown in equation (6).

$$\begin{cases} F_{tg} = \int_{-\frac{\pi}{2}}^{\frac{\pi}{2}} \frac{dF_t}{d\Psi} d\Psi = \frac{\pi}{4}\rho^2 F_p \sin\theta \cos^2\theta = \frac{\pi}{4} F_p \overline{a_g^2} \sin\theta \\ \\ F_{ng} = \int_{-\frac{\pi}{2}}^{\frac{\pi}{2}} \frac{dF_n}{d\Psi} d\Psi = \rho^2 F_p \sin^2\theta \cos\theta = F_p \overline{a_g^2} \sin\theta \tan\theta \end{cases} \qquad (6)$$

Meanwhile, the calculation formula of grinding force component can be expressed as equation (7).

$$\begin{cases} F_t = N_d F_{tg} = \frac{\pi}{4} N_d F_p \overline{a_g^2} \sin\theta \\ \\ F_n = N_d F_{ng} = N_d F_p \overline{a_g^2} \sin\theta \tan\theta \end{cases} \qquad (7)$$

Finally, the mathematical model of unit grinding force is shown as follows:

$$F_p = \frac{1}{2N_d \overline{a_g^2} \sin\theta}\left(\frac{4F_t}{\pi} + \frac{F_n}{\tan\theta}\right) \qquad (8)$$

Where, N_d is the number of dynamic effective grinding edges, $N_d = N_t \cdot l_c \cdot b$, N_t is the number of effective static grinding edges of per unit length on the surface of the grinding rod, l_c is the contact arc length between the grinding rod and the workpiece, b is the effective grinding width.

3.2 Experimental model of unit grinding force based on SiCp/Al composites

In the experiment, the abrasive particle shape of the grinding rod is regular dodecahedron, so θ is 60°. l_c is 1.5π mm and b is 3mm, so the formula of unit grinding force can be evolved as follows.

$$F_p = \frac{2\sqrt{3}}{9\pi N_t \overline{a_g^2}}\left(\frac{4F_t}{\pi} + \frac{F_n}{\sqrt{3}}\right) \qquad (9)$$

According to literature [21], the total number of particles in the grinding area per unit time is obtained as follows.

$$N_t = v_s b N_s \qquad (10)$$

Assuming that the material is uniformly removed when the grinding rod is grinding, then [22]

$$\overline{a_g^2} = \frac{a_p v_w}{N_s v_s l_c \tan\theta} \qquad (11)$$

By substituting formula (10) and formula (11) into formula (9), the experimental model of unit grinding force can be obtained as follows.

$$F_p = \frac{1}{3a_p v_w}\left(\frac{4F_t}{\pi} + \frac{F_n}{\sqrt{3}}\right) \qquad (12)$$

Because the actual F_n and F_t have been measured in this experiment, F_p can be calculated under certain conditions.

3.3 Experimental model of grinding force based on SiCp/Al composites

Over the years, scholars around the world have carried out a lot of research, published a lot of data, and discussed in detail the influence of grinding parameters on grinding force.Experimental formulas of grinding force have been put forward, which are almost all expressed in the form of power exponential function of grinding conditions. The form is as follows:

$$F = F_p a_p^{\alpha} v_s^{-\beta} v_w^{\gamma} b^{\delta} \tag{13}$$

Where, F is grinding force, F_p is the unit grinding force, b is the grinding width, α, β, γ and δ are exponents.

Then, the mathematical model of the experimental formula for end face grinding is:

$$F = F_p a_p^{x} v_s^{y} v_w^{z} \tag{14}$$

The experimental model for end face grinding is:

$$F = 28282 a_p^{0.86} v_s^{-1.06} v_w^{0.44} \tag{15}$$

Table 4 Experimental data of end face grinding force

Serial number	Grinding parameters			The level of coding				F/N	LnF
	a_p/mm	v_s/(m/min)	v_w/(m/min)	b_0	b_1	b_2	b_3		
1	0.01	30	0.003	+1	-1	-1	-1	4	1.39
2	0.01	35	0.004	+1	-1	+1	+1	7	1.95
3	0.02	30	0.004	+1	+1	-1	+1	12	2.48
4	0.02	35	0.003	+1	+1	+1	-1	10	2.30

In combination with the grinding parameters and experimental conditions of this experiment, regression processing is carried out on equation (13).

$$\ln F = \ln F_p + x \ln a_p + y \ln v_s + z \ln v_w$$
$$y = b_0 + b_1 x + b_2 y + b_3 z \tag{16}$$

Then, the grinding parameters are coded horizontally, with a large value of +1 and a small value of -1. The logarithm of the experimental value of grinding force is taken, as shown in Table 4. The solution are b_0=2.03, b_1=0.36, b_2=0.095 and b_3=0.185. The values of the three variables in equation (16) are successively solved as shown below.

$$x_1 = \frac{2(\ln a_p - \ln 0.02)}{\ln 0.02 - \ln 0.01} + 1 = 2.42 \ln a_p - 7.64$$

Assuming that A=2.42 and a=-7.64, x_1 and x_2 are as follows:

$$x_1 = A \ln a_p + a$$

$$x_2 = \frac{2(\ln v_s - \ln 35)}{\ln 35 - \ln 30} + 1 = -12.97 \ln v_s - 45.13$$

Assuming that M=-12.97 and m=-45.13, x_2 and x_3 are as follows:

$$x_2 = M \ln v_s + m$$

$$x_3 = \frac{2(\ln v_w - \ln 0.004)}{\ln 0.004 - \ln 0.003} + 1$$
$$= 2.71 \ln v_w - 37.39$$

Assuming that R=2.71 and r=-37.39, x_3 is as follows:

$$x_3 = R \ln v_w + r$$

By x_1, x_2 and x_3 into formula (16), the regression equation can be obtained as follows:

$$y = b_0 + b_1(A \ln a_p + a) + b_2(M \ln v_s + m)$$
$$+ b_3(R \ln v_w + r)$$
$$= (b_0 + b_1 a + b_2 m + b_{3r}) + b_1 A \ln a_p + b_2 M \ln v_s$$
$$+ b_3 R \ln v_w$$

$$F = e^{(b_0+b_1a+b_2m+b_3r)}a_p^{b_1A}v_s^{b_2m}v_w^{b_3R} \qquad (17)$$

Substituting the values of b_0, b_1, b_2, b_3, A, M, R, a, m and r into the following four equations, the cutting proportionality constant C_f and exponents x, y and z can be obtained as follows:

$$C_F = e^{(b_0+b_1a+b_2m+b_3r)} = e^{10.27} = 28853.89$$

$$x = b_1A = 0.36 \times 2.42 = 0.8712$$

$$y = b_2M = 0.095 \times (-12.97) = -1.1673$$

$$z = b_3R = 0.185 \times 2.71 = 0.5014$$

Substituting C_f ($\approx F_p$) and exponent x, y, and z values into equation (14), the experimental model of grinding force can be obtained as follows:

$$F = 28853.89a_p^{0.8712}v_s^{-1.1673}v_w^{0.5014} \qquad (18)$$

The three index values in formula (15) are 0.86, -1.06 and 0.44, which are basically the same as the obtained results of 0.8712, -1.1673 and 0.5014.

Table 5 Experimental data and relative errors of end face grinding forces

	a_p/mm	v_s/(m/min)	v_w/(m/min)	F_1/N	F_2/N	Δ
1	0.01	30	0.003	5.12	5.05	1.4%
2	0.015	35	0.004	29.01	28.5	1.7%
3	0.02	30	0.005	28.35	27.78	2.0%
4	0.025	35	0.006	43.01	42.32	1.6%
5	0.03	30	0.007	74.01	72.31	2.3%

Where, F_1 is the measured value, F_2 is the calculated value, Δ is the relative error of end face grinding forces as follows:

$$\Delta = \frac{F_1 - F_2}{F_1} \qquad (19)$$

Thus, the average relative accuracy of end face grinding force is shown as:

$$\Delta = \frac{\Delta_1 + \Delta_2 + \Delta_3 + \Delta_4 + \Delta_5}{5}$$
$$= \frac{1.4\% + 1.7\% + 2.0\% + 1.6\% + 2.3\%}{5}$$
$$= 1.8\%$$

Finally, the experimental data in Table 5 are used for experimental verification, and the average error is 1.8%, which is relatively small, so the accuracy of formula (16) can be verified.

4. Results and discussion

4.1 Experimental results

In this paper, SiCp/Al composites are grinding face by grinding rod. By collecting and sorting the normal grinding forces and tangential grinding forces, the grinding experimental study are carried out. The end grinding experiment is carried out on the high precision engraver CARVER 400, and the measurement of grinding force, grinding mode and device are described above. Because the axial force is small, it can be ignored in end face grinding. Therefore, only tangential grinding forces and normal grinding forces are measured. Fig. 5 shows the variation curve of tangential grinding forces and normal grinding forces with workpiece feed rate under dry grinding conditions. Fig. 6 shows the three-dimensional histogram of grinding forces at different workpiece feed rates and grinding depths.
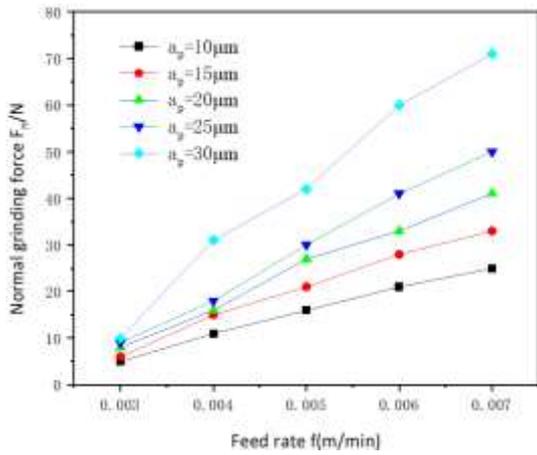
(a)Normal grinding force F_n
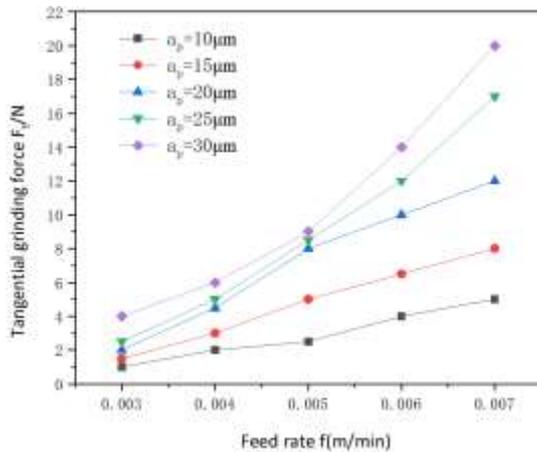
(b) Tangential grinding force F_t

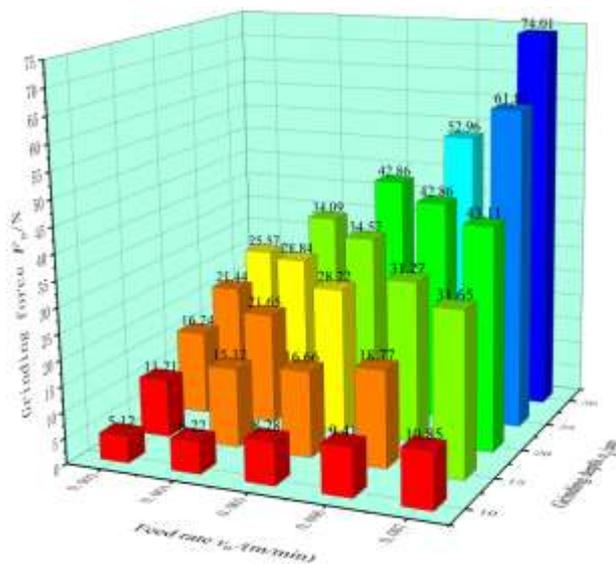Fig.5. Variation law of grinding force with workpiece feed rate under dry grinding condition

Fig. 6. The grinding force F_p under different workpiece feed rates and grinding depths

4.2 Influence of grinding parameters on grinding forces

4.2.1 Influence of feed rate on grinding force

Fig. 5 shows the change trend of the grinding force in the workpiece grinding experiment with the feed rate of the grinding rod in the dry grinding process. The feed rate is between 0.003 m/min and 0.007 m/min. It is founded that tangential grinding forces and normal grinding forces increase with the increase of rod feed rate under dry grinding conditions. The two kinds of grinding forces change roughly the same law, and the normal grinding force is greater than the tangential grinding force. As can be seen from Fig. 6, the grinding force also increases with the increase of feed rate, and the influence degree of feed rate on grinding force is second only to grinding depth.

Under the conditions of dry grinding process, the effect of feed rate on grinding force is as follows.Under the condition of the same grinding depth, the tangential grinding forces and normal grinding forces continue to increase with the increase of the feed rate. When the feed rate increases from 0.003 m/min to 0.007 m/min, the increase amplitude of the tangential grinding forces and the normal grinding forces increases first and then decreases. When the grinding depth is 20 μm and the feed rate is from 0.003 m/min to 0.005 m/min, the tangential grinding force increases from 2 N to 8 N with a large increase range. In the same period, the value of normal grinding force increases from 8 N to 27 N, and the increase is also large. When the feed rate is from 0.005 m/min to 0.007 m/min, the value of tangential grinding force increases from 8 N to 12 N, and its increase is small. In the same period, the value of normal grinding force increases from 27 N to 41 N, and the increase is also small. With the increase of the feed rate, the cutting thickness of a single abrasive particle increases, and the number of abrasive particles participating in the cutting also increases, which makes the normal grinding force and tangential grinding force increase. On the other hand, with the increase of feed rate, the impact frequency of hard particles and diamond abrasive particles increases in unit time, which makes the tangential grinding force and normal grinding force increase simultaneously. As the feed rate continues to increase, the cutting thickness of abrasive particles

continues to increase. At the same time, the increase of brittle spalling of reinforced SiC particles in SiCp/Al composites means that the material is more removed by brittle fragmentation, so the increase of grinding force becomes smaller.

4.2.2 Influence of grinding depth on grinding force

It can also be seen from Fig. 5 that both the tangential grinding forces and the normal grinding forces increase with the increase of grinding depth in dry grinding process. When the feed rate is 0.007 m/min, the normal grinding force increases from 50 N to 71 N with the largest increase in the process of grinding depth of 25 ~ 30 μm. Under the condition of the same feed rate, the tangential grinding force increases from 12 N to 17 N when the grinding depth is from 20 μm to 25 μm.

There are two reasons to explain the increase of grinding force with grinding depth as follows:

(1) When the grinding depth increases, the maximum undeformed cutting thickness of a single abrasive grain increases, the contact arc length between the grinding rod and the workpiece increases, and the number of abrasive grains in actual work increases, so the grinding force increases.

(2) When the grinding depth increases, the friction between the binder, the grinding shoulder and the surface of the workpiece increases, so the grinding force also increases. Among them, the tangential grinding force increases more.

As can be seen from Fig. 6, with the grinding depth increasing, the grinding force will also increase, and the grinding depth has the greatest influence on the grinding force.

4.2.3 Influence of grinding conditions on grinding forces

For mesoscopic grinding of aluminum matrix composites with high volume fraction SiC particles as reinforcement, most scholars took the dry grinding method [23] to grind the workpiece, in order to reduce errors and improve accuracy. Therefore, the characteristics of the tangential grinding force and the normal grinding force were analyzed under dry grinding conditions in this paper. The range of tangential grinding force is 5 ~ 20 N, and the range of normal grinding force

is 25 ~ 71 N in dry grinding. Under dry grinding conditions, because there is no cooling measures, the workpiece surface will gradually rise with the grinding process, and the unit volume of the material will increase, which will generate internal stress and induce a lot of displacement and dislocation in the material, and then increase the strength of Al matrix. In addition, the internal defects (pores and cracks) of SiCp/Al composites are closed due to the volume expansion during the heating process. It is because the hardness and strength of the workpiece material have been improved and the grinding process without lubricating fluid to reduce friction, so the dry grinding process will obtain greater grinding force.

4.3 The variation rule of grinding component force ratio under dry grinding conditions

The larger the grinding component force ratio is, the greater the degree that the normal grinding force is greater than the tangential grinding force. In this experiment, the direction of normal grinding force is opposite to the direction of rod groove grinding, and the difference between the two values is too large, which leads to the decrease of the surface quality of processed SiCp/Al material. Therefore, in order to lay a foundation for revealing the grinding surface mechanism more comprehensively, the variation law of grinding component force ratio of SiCp/Al composites was obtained by collecting and analyzing the grinding forces. The grinding component force ratio is the numerical ratio of the normal grinding force and the tangential grinding force. The calculation formula of the grinding force component ratio is shown in equation (20).

$$C_f = F_n / F_t \tag{20}$$

The SiCp/Al composite material adopted in this experiment is characterized by high hardness and strong brittleness, so the grinding component force ratio is large in the grinding process, and the normal grinding force is far greater than the tangential grinding force. The tangential grinding force consists of the tangential cutting force and the tangential friction force. The cutting

force can directly remove the machinable surface of the material, while most of the friction force hinders the removal of the machinable surface of the material. Fig. 7 shows the variation law of grinding component force ratio with grinding depth at different feed rates under dry grinding conditions.
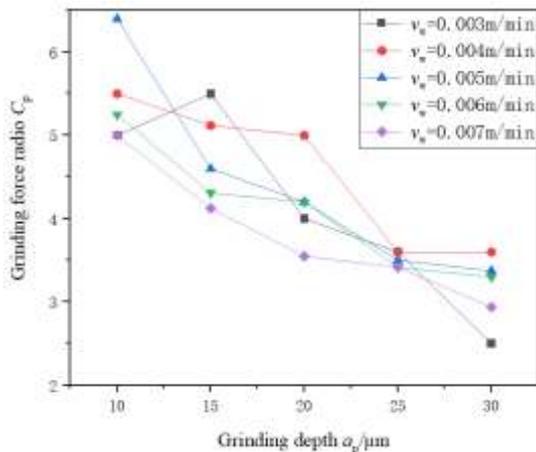

Fig. 7. Variation rule of grinding component force ratio

As can be seen from Fig. 7, the range of C_f is 2.5 ~ 6.4 under the conditions of feed rate of 0.003 ~ 0.007 m/min and grinding depth of 10 ~ 30 μm. The large range of variation reflects the hard and brittle characteristics of SiCp/Al composites. With the increase of grinding depth, the grinding component force ratio shows a downward trend. Therefore, with the increase of grinding depth, the friction area on the side of the grinding rod increases, which leads to the increase of friction force. In addition, dry grinding debris is difficult to discharge, which will cause the plug of the grinding rod is also the reason of dry grinding tangential friction. Under the condition of the constant tangential cutting force, the tangential grinding force increases. Similarly, the normal grinding force is also composed of the normal grinding force and the normal friction force, but the increase of the grinding side area will only lead to a small change in the normal friction force (basically unchanged), so the normal grinding force is basically unchanged. According to equation (17), under the condition that the normal grinding force remains unchanged, the tangential grinding force increases to lead to a smaller grinding component force ratio.

5. Conclusions

(1) An experimental platform for grinding the end face of the grinding rod is built, and different experimental parameters are selected to carry out the grinding experiments. Several groups of grinding force values are measured during the grinding process. The results are analyzed and the mathematical models of unit grinding force and grinding force were established. The accuracy of the model is verified by designing experimental parameters, and the average error is 1.8%.

(2) Under the conditions of dry grinding process, the influence of the three grinding parameters on the normal grinding force and tangential grinding force is: grinding depth > feed rate > spindle speed. When the grinding depth is constant, the normal grinding force and the tangential grinding force continue to increase with the increase of feed rate. With the increase of grinding depth, the two grinding forces continue to increase when the feed rate is constant.

(3) In this experiment, under dry grinding conditions, the range of the tangential grinding force is 5 ~ 20 N, the range of the normal grinding force is 25 ~ 71 N, and the grinding force changes greatly. The one of the reasons for the above phenomenon is that there is no cutting fluid lubrication in the grinding process, the workpiece is heated up. At this point, the increase in the unit volume of the material will generate internal stress and induce a large number of displacement and dislocation, which in turn will increase the strength of Al matrix. The other reason is that the internal defects (pores, cracks) of SiCp/Al composites are closed due to the volume expansion during the heating process. At this time, the hardness and strength of the workpiece material is improved greatly, so the grinding force changes greatly.

(4) When the feed rate is 0.003 ~ 0.007 m/min and the grinding depth is 10 ~ 30 μm, the range of C_f is 2.5 ~ 6.4, which the wide variation range reflects the hardness and brittliness of SiCp/Al composites. With the increase of grinding depth, the grinding component force ratio of SiCp/Al composites shows a trend of decline.

Conflicts of interest/Competing interests

The authors have declared that no conflict of interest exists.

Availability of data and material

The data used to support the findings of this study are available from the corresponding author upon request.

Code availability

Ethical Approval

This research project has been approved by the Ethics Committee of Liaoning University of Technology.

Consent to Participate

I solemnly declare that the paper "Study on removal mechanism and surface quality of high volume fraction SiCp/Al composites based on meso-scale" presented by us is the result of our research. This paper does not contain any work published or written by any other individual or group, except for the content specifically noted and cited in the paper. I fully realize that the legal consequences of this statement shall be borne by me.

Consent for publication

that the work described has not been published before;

that it is not under consideration for publication elsewhere;

that its publication has been approved by all co-authors, if any;

that its publication has been approved by the responsible authorities at the institution where the work is carried out.

The Author agrees to publication in the Journal indicated below and also to publication of the article in English by Springer in Springer's corresponding English-language journal. The copyright to the English-language article is transferred to Springer effective if and when the article is accepted for publication. The author warrants that his/her contribution is original and that he/she has full power to make this grant. The author signs for and accepts responsibility for releasing this material on behalf of anyand all co-authors. The copyright transfer covers the exclusive right to reproduce and distribute the article, including reprints, translations,

photographic reproductions, microform, electronic form or any other reproductions of similar nature. After submission of the agreement signed by the corresponding author, changes of authorship or in the order of the authors listed will not be accepted by Springer. Journal: The International Journal of Advanced Manufacturing Technology, chemical samples Names of ALL contributing authors：Guangyan Guo, Qi Gao, Quanzhao Wang, and Shichao Pan.

Authors' contributions

Guo did all the grinding experiments and wrote the papers. Gao guided Guo to revise the paper. Wang made a parameter measurement of the materials used in this experiment. Pan performed regular segmentation of the SiCp/Al composites. All authors read and approved the manuscript.

References

1. Wang JF, Zhao JL, Chu KY. Simulation Study on Cutting Force of SiCp/A1 Composite. Journal of System Simulation, 2018, 30(4): 1566-1571.

2. Chen JP, Gu L,He GJ. A review on conventional and nonconventional machining of SiC particle-reinforced aluminium matrix composites. Advances in Manufacturing, 2020, 8(3): 279-315.

3. Xiang DH, Shi ZL, Feng HR. Finite element analysis of ultrasonic assisted milling of SiCp/Al composites. The International Journal of Advanced Manufacturing Technology, 2019, 105(7-8): 3477-3488.

4. Xiang JF, Xie LJ, Gao FN. Diamond tools wear in drilling of SiCp/Al matrix composites containing Copper. Ceramics International, 2018, 44(5): 5341-5351.

5. Zhao X, Gong YD, Liang GQ. Face Grinding Surface Quality of High Volume Fraction SiCp/Al Composite Materials. Chinese Journal of Mechanical Engineering, 2021, 34(1).

6. Zhou M, Zheng W. A model for grinding forces prediction in ultrasonic vibration assisted grinding of SiCp/Al composites. The International Journal of Advanced Manufacturing Technology, 2016.

7. Sakthi S, Ramar M. INVESTIGATION OF SURFACE GRINDING CHARACTERISTICS OF

AL/SIC/AL2O3 COMPOSITE USING GREY RELATIONAL ANALYSIS. International Journal on Design & Manufacturing Technologies, 2016.

8. Yin GQ, Wang D, Cheng J. Experimental investigation on micro-grinding of SiCp/Al metal matrix composites. The International Journal of Advanced Manufacturing Technology, 2019.

9. Yu XL, Huang ST, Xu LF. ELID grinding characteristics of SiCp/Al composites. The International Journal of Advanced Manufacturing Technology, 2016.

10. Huang ST, Yu XL. A study of grinding forces of SiCp/Al composites[J]. The International Journal of Advanced Manufacturing Technology, 2018.

11. Zhao L. Study on simulation and experiment of grinding force of SiCp/Al composite material.Shenyang Ligong University, 2012.

12. Duan CZ, Che MF, Sun W, Yin WD. Study of Cutting Force on High Volume Fraction SiCp/Al Composites. Modular Machine Tool & Automatic Manufacturing Technique, 2019(02):1-4.

13. Pramanik A, Zhang LC, Arsecularatne JA. Prediction of Cutting Force in Machining of Metal Matrix Composites. International Journal of Machine Tool & Manufacture, 2006, 46(14):1795-1803.

14. Bian WL, Fu YC, Xu JH. High-Speed Milling-Force Model for SiCp/Al Composites. Aeronautical Manufacturing Technology, 2012, (03):92-95.

15. Han DR, Wang DZ, Liu HM. Research on the Cutting Force Properties of Machining SiCp/2024 Composites. Chinese High Technology Letters, 2001, (07):94-96.

16. Liu Q, Wang JF, Zhao JL, Chu KY, Liu SX. Modeling of cutting forces in turning of SiCp/Al composites. Chinese Journal of Construction Machinery, 2018, 16(03):211-215.

17. Zhang FL, Li MC, Wang J. Effect of arraying parameters on dry grinding performance of patterned monolayer brazed CBN wheel. The International Journal of Advanced Manufacturing Technology, 2020, 107(5):2081-2089.

18. Wang YS, Xiu ST, Dong L, Sun C. Study on strengthened layer of workpiece in prestress dry grinding. The International Journal of Advanced Manufacturing Technology, 2016, 90(5-8).

19. Qu MN, Jin T, Xie GZ, Cai R, Yi J, Lu AG. Thermal damage control for dry grinding of MgO/CeO2 glass ceramic. International Journal of Advanced Manufacturing Technology, 2019, 105(7-8).

20. Wang YS, Xiu SC, Sun C. Study on surface topography of workpiece in prestress dry grinding. International Journal of Advanced Manufacturing Technology, 2017, 90(1):1225-1233.

21. Younis MA, Alawi H. Probabilistic analysis of the surface grinding process. Trans CSME, 1984, 8(4):208-213.

22. Gu P, Zhu CM, Tao Z, Yu YQ. A grinding force prediction model for SiCp/Al composite based on single-abrasive-grain grinding. International Journal of Advanced Manufacturing Technology, 2020, 109(5-8).

23. Duan CZ, Che MF, Sun W, Wei B, Liu YM. Influence of different cooling and lubrication methods on tool wear in machining SiCp/Al composites. Acta Materiae Compositae Sinica, 2019,36(05):1244-1253.